Received April 2001
Accepted December 2001

Numerical simulation of the performance of a vortex controlled diffuser in low Reynolds number regime

S. Chakrabarti
Department of Mechanical Engineering, Bengal Engineering College, Deemed University, West Bengal, India
S. Ray and A. Sarkar
Department of Mechanical Engineering, Jadavpur University, Kolkata, India

Keywords *Vortex dynamics, Pressure, Efficiency*

Abstract *In this paper, the performance simulation of a vortex controlled diffuser (VCD) has been carried out in low Reynolds number regime. The two-dimensional steady differential equations for conservation of mass and momentum has been solved for the Reynolds number ranging from 20 to 100, aspect ratio for 2 and 4, and bleed fraction for 2 per cent, 5 per cent and 10 per cent. The effect of each variable on the diffuser efficiency and the stagnation pressure has been studied in detail. From the study, it has been revealed that when the bleed is incorporated, the VCD behaves in a completely different manner from that of a sudden expansion as far as the variation of total pressure along the diffuser is concerned. For a given Reynolds number and aspect ratio, the diffuser efficiency has been noted to be increasing with increase in bleed fraction. VCD with an area ratio of around two has been found to be most suitable. The top corner has been noted to be the most desirable location of the bleed slot for the best performance of the VCD for the considered Reynolds number regime.*

Nomenclature

A = Area at any section
A^* = Aspect ratio or area ratio, given by A_2/A_1
dA = Elemental area
B = Bleed fraction, given by $\dot{m}_b/\dot{m}_1$
L_b = Length of the bleed slot
L_i = Inlet length (i.e. length between throat and iniet section)
L_{ex} = Exit length (i.e. length between exit section and throat)
L_R = Reattachment length
$\dot{m}$ = Mass flow rate
p = Static pressure
$\bar{p}$ = Average static pressure
$\bar{p}^*$ = Dimensionless average static pressure
p_s = Stagnation pressure
$\bar{p}_s$ = Average stagnation pressure
p_s^* = Dimensionless stagnation pressure
$\bar{p}_s^*$ = Dimensionless average stagnation pressure
p_w^* = Dimensionless wall pressure
Re = Reynolds number
s^* = Dimensionless distance along the wall
u,v = Velocity components in x and y directions of a Cartesian co-ordinate
V = Average velocity

International Journal of Numerical Methods for Heat & Fluid Flow, Vol. 12 No. 3, 2002, pp. 224-240.

DOI 10.1108/09615530210422884

$\bar{V}$ = Velocity vector
W = Width of the channel
x,y = Cartesian co-ordinates
z = Distance of bleed slot on the horizontal side from throat
η_{diffuser} = Diffuser efficiency
μ = Dynamic viscosity
ρ = Density
Ψ = Stream function

Subscripts
1, i = Inlet
2 = Exit
b = Pertaining to bleed zone

1. Introduction

Massive improvements, in recent years, in the technology of different components of air-craft gas turbine have placed a greater emphasis upon the requirement and consequently the development of short and efficient diffusers which are to be placed between the compressor and the combustor that has the primary function of reducing air velocity to ensure efficient combustion at a low pressure loss. In addition, the inlet flow distribution is also a matter of utmost significance for a particular engine operating condition. While discussing the configuration of a diffuser, the first choice that comes to mind is a 'sudden expansion' configuration. Recently, the present authors carried out a detail numerical analysis on the performance study of a back-step, as diffuser (Chakrabarti *et al.*). Although the study was mainly limited to low-Re regime, it did reveal several outstanding features. For example, its efficiency as a diffuser was found to be typically dependent on aspect ratio, inlet length, type of inlet velocity profile and Reynolds number. It was further observed that, in the range of parameters considered, maximum diffuser efficiency was achieved for an aspect ratio of around two; in addition, the efficiency vs. aspect ratio curve exhibited a near-flat characteristics on either side of the optimum value of the aspect ratio; while this may be considered to be a desirable feature, the serious disadvantage was that the length required for the diffusion of inlet kinetic energy strongly depended on the flow Reynolds number. Consequently, variable geometry diffusers were designed to subvert the dominance of the above problem; however this was associated with considerable increase in mechanical complexity. A simple and at the same time viable alternative could be the deployment of a vortex controlled diffuser (VCD) that has some of the advantages of the back-step as diffuser. However, the major advantage claimed in favour of the VCD is that the length of the diffusion zone can be effectively controlled by employing a suction at the convex corner of the step. The bleed fluid is proposed to be used for turbine blade cooling.

From literature, it appears that the first work on the performance study of VCD was reported by (Heskestad, 1961; Heskestad, 1968). In his experimental work, Heskestad employed a suction slot at the convex discontinuity of a step expansion in a circular pipe. The suction gap is formed by the space between two 30° included-angle Wedges. He considered two area ratios with flow Reynolds number varying between 2×10^4 and 20×10^4. He identified a critical suction rate below which the suction flow is taken primarily from the separated region in the shade of the step. He further indicated that the flow expansion not

only depended on the suction rate but also on the geometric configuration of the suction gap. As far as the efficiency of the diffuser is concerned, he stressed that suction power must be taken into consideration. He compared his results with that of a conical diffuser and concluded that better pressure recoveries might be obtained with a suction diffuser than a conical diffuser particularly when the dimensionless length of the diffuser were less than five. A contemporary work by (Ringleb, 1955) explained the aerodynamic design of cusps in the diffuser walls so that the vortices could be located in them. His objective was to reduce the boundary shear stress experienced by the flow in the region of high adverse pressure gradients. This was to be achieved by replacing the fixed wall with a vortex, rotating in the direction of flow. However, difficulty was experienced in retaining a stable vortex system Following the work of Heskestad, Beatty (1970) found that the quantity of bleed required could be maintained at reasonable proportions by locating a fence directly downstream of the vortex region. Adkins (1975) carried out extensive experimental research to obtain a satisfactory vortex chamber arrangement that would have an acceptable minimum bleed requirement and a good static pressure recovery with an equivalent included angle of 30°. In his experimental setup, he allowed the diffuser mainstream to be exhausted directly to the atmosphere and the bleed flow was extracted by way of a suction pump. The expression of diffuser efficiency, as used by Adkins, however, attracted criticism for reasons to be described in detail by the present workers later. His results indicated the potential or prospect of VCD in future precombustor applications. Sullerey *et al.* (1992) carried out investigations to evaluate experimentally the effect of various vopex controlled diffuser geometrical parameters, suction rates and diffuser inlet velocity profile on the diffuser exit flow distribution and pressure recovery. In their work, they considered both the VCD and the hybrid diffuser. They also used the same expression of diffuser efficiency as outlined by Adkins. They concluded that hybrid diffusers require appreciably lower bleed rates than VCD to achieve high performance. It was also indicated that the hybrid diffuser performs better than the VCD in some other important aspects as well like lower value of the co-efficient of vortex chamber depression and more uniform diffuser outlet velocity profile.

The foregoing represents a brief survey of the experimental observations on VCD. From the survey, it is evident that while different fluids had been used during the experiments at different values of Reynolds number (mostly in the high Re-regime), there exists a void as far as the numerical prediction of the performance of a VCD at low and medium values of Re is concerned. A low Re performance analysis is considered important in view of the fact that the temperature of air at inlet to the diffuser could be in the region of 750 K and the viscosity is very high. From the survey it is also apparent that the variation of the position and size of the suction slot has not been explored. In this work then, an extensive endeavour has been made to numerically predict the performance

of a VCD at low Re-regime; in addition, the effect of such important parameters as percentage bleed; variation of position of suction slot on typical diffuser properties have been investigated.

In this article, a brief mathematical formulation has been presented in Section 2 The governing equations along with their respective boundary conditions and an overview of the numerical method have been reported in the section. The important results have been discussed in detail in Section 3. In the section, the effects of flow Reynolds number, aspect ratio, bleed fraction and the variation of location of bleed slot on the wall pressure, average static and stagnation pressures, diffuser efficiency have been presented. The major conclusions are reported in Section 4.

2. Mathematical formulation

2.1 Governing equations

A schematic diagram of the computational domain is illustrated in Figure 1. The flow under consideration is assumed to be steady, two-dimensional and laminar. The fluid is considered to be incompressible and obeys Newton's law of viscosity. The following dimensionless variables are defined to obtain the governing conservation equations in the non-dimensional form:

Lengths: $x^* = x/W_1, y^* = y/W_1, L_R^* = L_R/W_1, L_{\text{ex}}^* = L_{\text{ex}}/W_1, L_b^* = L_b/W_1, z^* = z/W_1$

Velocities: $u^* = u/V_1, v^* = v/V_1$

Pressure: $p^* = (p + \rho g y)/\rho V_t^2$

With the help of these variables, the mass and momentum conservation equations are written as follows,

$$\frac{\partial u^*}{\partial x^*} + \frac{\partial v^*}{\partial y^*} = 0 \tag{1}$$

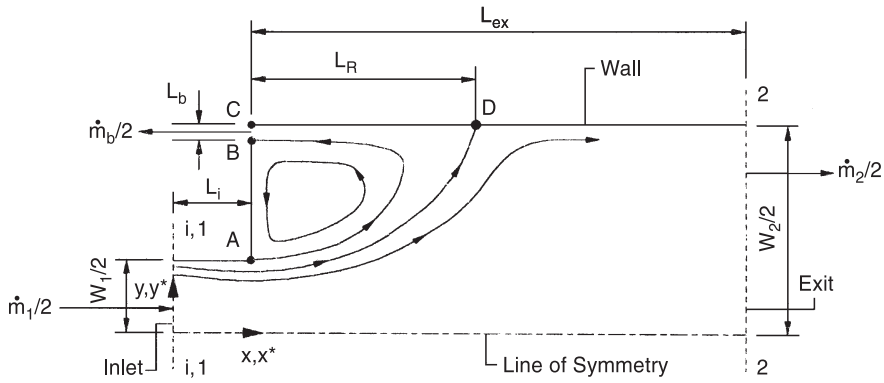

Figure 1.
Schematic Diagram of the computational domain

$$\frac{\partial(u^*u^*)}{\partial x^*}+\frac{\partial(v^*u^*)}{\partial y^*}=-\frac{\partial p^*}{\partial x^*}+\frac{1}{\mathrm{Re}}\left[\frac{\partial}{\partial x^*}\left(\frac{\partial u^*}{\partial x^*}\right)+\frac{\partial}{\partial y^*}\left(\frac{\partial u^*}{\partial y^*}\right)\right] \quad (2)$$

$$\frac{\partial(u^*v^*)}{\partial x^*}+\frac{\partial(v^*v^*)}{\partial y^*}=-\frac{\partial p^*}{\partial y^*}+\frac{1}{\mathrm{Re}}\left[\frac{\partial}{\partial x^*}\left(\frac{\partial y^*}{\partial x^*}\right)+\frac{\partial}{\partial y^*}\left(\frac{\partial v^*}{\partial y^*}\right)\right] \quad (3)$$

where, the flow Reynolds number, $\mathrm{Re}=\rho V_1 W_1/\mu$.

2.2 Boundary conditions

Five different types of boundary conditions are applied to the present problem. They are as follows,

(1) At the walls: No slip condition is used, i.e., $u^*=0$, $v^*=0$.

(2) At the bleed slot: When the slot is on the vertical side of the VCD, the negative uniform axial velocity is specified and the transverse velocity is set to zero, i.e., $u^*=$ specified, $v^*=0$, and for the slot on the horizontal side, the axial velocity is set to zero and an uniform transverse velocity is specified.

(3) At the inlet: Axial velocity is specified for fully developed flow condition and the transverse velocity is set to zero, i.e., $u^*=1.5[1-(2y^*)^2]$, $v^*=0$.

(4) At the exit: Fully developed condition is assumed and hence gradients are set to zero, i.e., $\partial u^*/\partial x^*=0$, $\partial v^*/\partial x^*=0$.

(5) At the line of symmetry: The normal gradient of the axial velocity and the transverse velocity are set to zero, i.e., $\partial u^*/\partial y^*=0$, $v^*=0$.

2.3 Numerical procedure

The partial differential Equations (1)–(3) are discretised by a control volume based finite difference method. Power law scheme is used to diseretise the convective terms (Patankar, 1980). The discretised equations are solved iteratively by SIMPLE algorithm, using line-by-line ADI method. The convergence of the iterative scheme is achieved when the normalised residuals for mass and momentum equations summed over the entire calculation domain fall below 10^{-8}.

In the present computation, the flow is assumed to be fully developed at the exit and hence, the exit is chosen far away from the throat. For all the calculations, the inlet length and the exit length are considered to be 1 and 50 respectively. The distribution of grid nodes is non-uniform in both co-ordinate directions allowing higher grid node concentrations in the region close to the step and walls of the duct. Solutions are obtained with different grid densities for $A^*=2$ and $\mathrm{Re}=100$. The pressure distribution along the wail has been studied as a function of numerical grid to achieve a grid independent solution.

Finally, when the bleed slot has been placed on the vertical side of the VCD, for inlet section 17×13 grid has been considered, while 85×35 grid is chosen for the exit section in x and y directions respectively. When the bleed slot has been provided on the horizontal side, the grids in the inlet and exit sections have been considered as 17×13 and 95×31 respectively.

In addition to the above, the results of the grid independence test is quantified and the outcome of such an exercise, in terms of the magnitude and location of ψ_{max}. is described in Table I. During the study of the grid-independence test, the discritization of the inlet section was held constant at 17×13 grid i.e, 17 nodes along the x-direction and 13 nodes along the y-direction. This appears to be reasonable in view of the fact that it is the after-throat section that is of prime importance as far as the performance of the VCD is concerned. So, any grid independence test must be extensively performed over this region.

Accordingly, meshes of different sizes have been used for the exit section for the given values of parameters indicated in Table I. It is seen that the value for 85×35 grid matches exactly with 105×35 or 105×45 grid. Slight discrepancy, as far as the location of the ψ_{max} is concerned, is noted – however, this is unavoidable in view of the changes in mesh sizes. The results strongly recommend the use of 85×35 grid for the exit section without any significant loss of accuracy.

Grid nodes		
Inlet	Exit	ψ_{max} (x,y)
	105×45	0.5086 (1.244, 0.595)
	105×35	0.5086 (1.244, 0.587)
	105×25	0.5081 (1.244, 0.622)
	85×45	0.5087 (1.337, 0.595)
	85×35	0.5086 (1.337, 0.587)
17×13	85×25	0.5085 (1.337, 0.622)
	65×45	0.5095 (1.276, 0.595)
	65×35	0.5095 (1.276, 0.587)
	65×25	0.5091 (1.276, 0.622)

Table I. Results of grid independence test for $B = 10\%$

3. Results and discussion

The important results of the present study are reported in this section. The parameters those affect the flow characteristics are identified as,

(1) Reynolds number, $20 \leq \mathrm{Re} \leq 100$.

(2) Aspect ratio, $A^* = 2$ and 4.

(3) Bleed fraction, $B = 2$ per cent, 5 per cent and 10 per cent.

3.1 Variation of static pressure along solid boundary of VCD

We begin this chapter with a brief discussion on the variation of static pressure along the solid boundary of the VCD. The distribution of static pressure along the wail of the VCD is important in view of the fact that such distributions can be readily compared with the experiment. Figure 2 describes the typical result when the VCD is operated without bleed and with a bleed of 2 per cent, 5 per cent and 10 per cent located at the top corner on the vertical wall while the aspect ratio and the flow Reynolds number are held constant at 2 and 100 respectively. The genera1 trend in the variation of static pressure at the wall with distance from the inlet section is similar to that of sudden expansion (Chakrabarti *et al.*) excepting the region of suction slot where there is very sharp variation of pressure as shown in the inset. The positions of throat (A) and the extent of suction slot (B-C) are also marked on the inset. The behaviour i.e. the variation of static pressure along the vertical wall can be explained in the following manner: after the initial drop of static pressure along the inlet

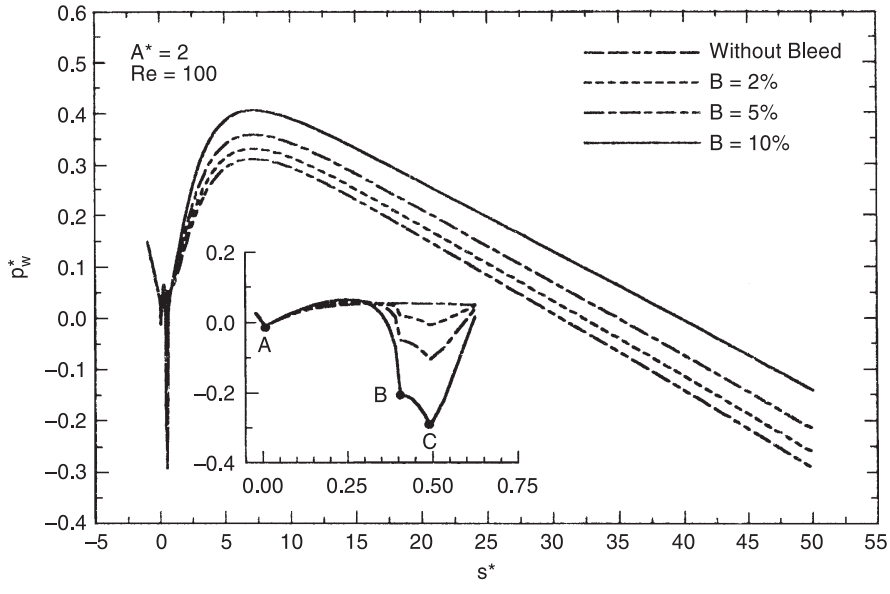

Figure 2.
Variation of Wall Pressure with distance along the wall

length, the fluid at the throat begins to experience a static pressure rise (as shown in the inset) presumably without being aware of the existance of the slot at the other end of the vertical wall. In fact, had it been the case of a sudden expansion without the provision of any bleeding arrangement, a continuous increase in static pressure up to the point of maximum diffusion would have been expected. The presence of the slot not only arrests the increasing trend but also brings down the pressure (point B). At the slot, an uniform outlet velocity profile is prescribed. Now at point C, the horizontal suction velocity is augmented to the greatest extent because of the near horizontal pattern of the stream line approaching point C from the interior of the VCD; the augmentation reduces as point B is approached. This in essence points to the fact that although a slug flow outlet condition has been impressed on the suction slot, a near half-trapezoid type of velocity distribution is, in effect, created there. The remainder part of pressure rise is achieved due to diffusion of fluid kinetic energy that is impressed on the wall; this is thereafter followed by drop in static pressure because of the presence of friction. As the bleed decreases, the magnitude of the static pressure variation at the wall in the region of suction slot diminishes because the arrest of increasing trend in static pressure due to presence of suction slot will decrease.

3.2 Variation of stagnation pressure along the centre line

The variation of stagnation pressure along the centre line is shown in Figure 3. For reasons unambiguously stated in Chakrabarti *et al.*, it seemed logical to expect a continuously decreasing tendency of the stagnation on pressure along the centre line of the VCD. It was reasoned that since symmetry. conditions are assumed to prevail in the present situation, the centre line of the VCD could be considered as a stream line and in absence of any energy transfer in the form of heat or work, stagnation pressure is bound to fall along the stream line for actual fluids. In fact the same trend is obtained in Figure 3. The three curves correspond to different bleed fractions for $Re = 100$, and an aspect ratio of 2. It is seen that upto the throat, the variation of stagnation pressure along the centre line for these three cases are same implying that at $Re = 100$ the flow along the inlet length is not influenced by the bleeding at the throat. However, from the throat onwards, the three curves are different. It is seen that greater stagnation pressure drop occurs for the lower bleed fraction. In the figure, the behaviour of the stagnation pressure variation for sudden expansion, but with no bleed, is also shown. Clearly, at any given location, with increase in bleed there is an increase in stagnation pressure. This can be explained by the fact that, due to continuity requirement, if the mass flow rate through the post-throat section is decreased, the velocity is reduced i.e. the greater the bleed the smaller will be the velocity. Hence, for a greater bleed, the lesser will be the kinetic contribution towards the stagnation pressure. However, the static pressure recovery will be more (refer Figure 4), since with greater bleed, a

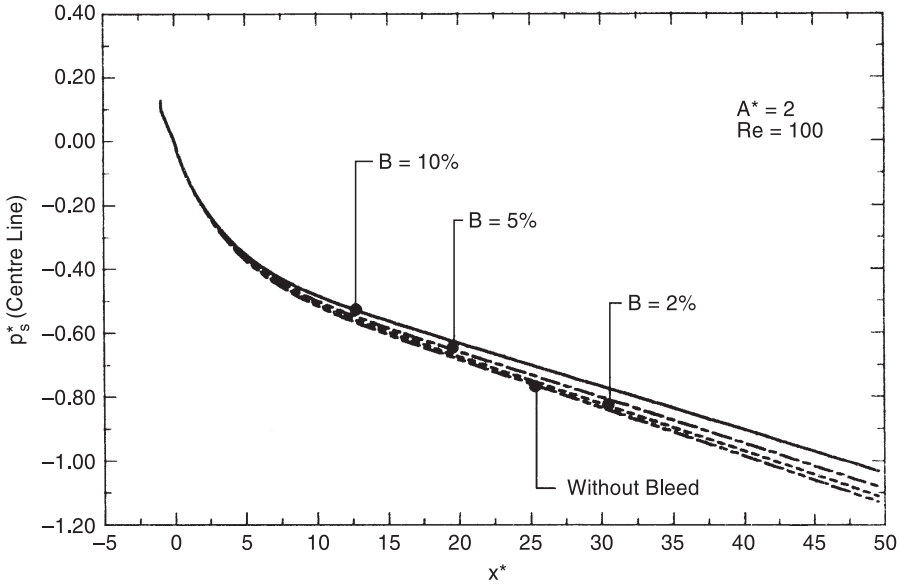

Figure 3.
Variation of centre line stagnation pressure with axial distance

greater mass of the low energy fluid from the recirculating zone goes out – thus resulting in a net gain in stagnation pressure, for higher bleed, at any given location.

3.3 Variation of average stagnation pressure along the length of the VCD

The calculation of average stagnation pressure at any given section, should take into consideration the direction of the velocity vector particularly for a flow situation like the present case where the flow is of recirculating type. The following expression has been considered for calculation of average stagnation pressure at a location:

$$\bar{p}_e = \frac{\int A_e \left(p_e + \frac{1}{2}\rho V_{\bar{e}}^2 \right) u_e dA_e}{\int A_e u_e dA_e} \tag{4}$$

where the subscript 'e' refers to the plane of measurement. The detail has been described in (Chakrabarti *et al.*). Typical variation for 2 per cent, 5 per cent and 10 per cent bleed, without bleed. aspect ratio of 2 and Reynolds number of 100 is described in Figure 5. As is seen therefrom for the case of bleed, the average stagnation pressure decreases in an expected manner from the inlet to the throat. At the throat it experiences a steep rise – a trend which was absent in the case of sudden expansion without any bleed. This behaviour can be readily

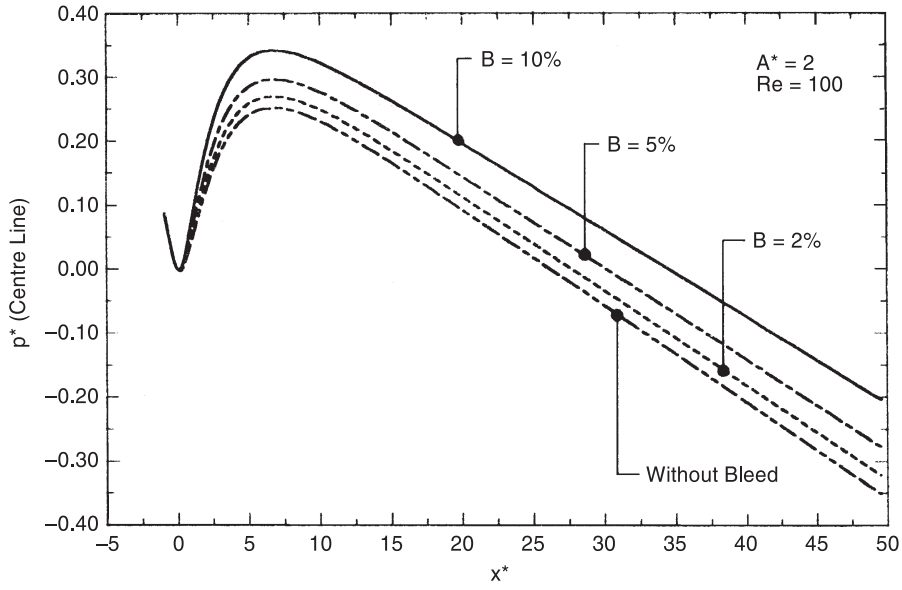

Figure 4.
Variation of centre line pressure with axial distance

explained by noting that the denominator in the above equation represents a net mass flow across a given section. At the throat, this denominator suddenly experiences a decrease in the value due to the presence of bleed section there. The stagnation pressure, however, still drops but this spatial variation of stagnation pressure across the throat is more than offset by the sudden decrease of net mass flow at the throat section and hence the steep rise in average stagnation pressure. To consolidate the reasoning cited above, it is further noted that while, for sudden expansion with no bleed, no such jump was recorded (Chakrabarti *et al.*), similar steep rise of much smaller magnitude was observed when the bleed was reduced (refer Figure 5). This strongly endorses the reasoning that the greater the bleed, the steeper will be the rise of average stagnation pressure close to the throat. Since the recirculating fluid has been identified to play a crucial role in rather sharp variations of average stagnation pressure, one may expect that in the post recirculation zone, the average stagnation pressure will decrease steadily. Figure 5 confirms this expectation. However, the steep decrease of average stagnation pressure is confined in the zone bounded by the throat and the end of recirculation zone.

3.4 Average static pressure rise along the length of the diffuser

From the diffuser point of view, the static pressure rise is of prime importance and the objective should be to ensure a high static pressure rise. Again this should be achieved with minimum stagnation pressure loss and in addition, the length of the diffuser should be as small as possible. In the present work, the

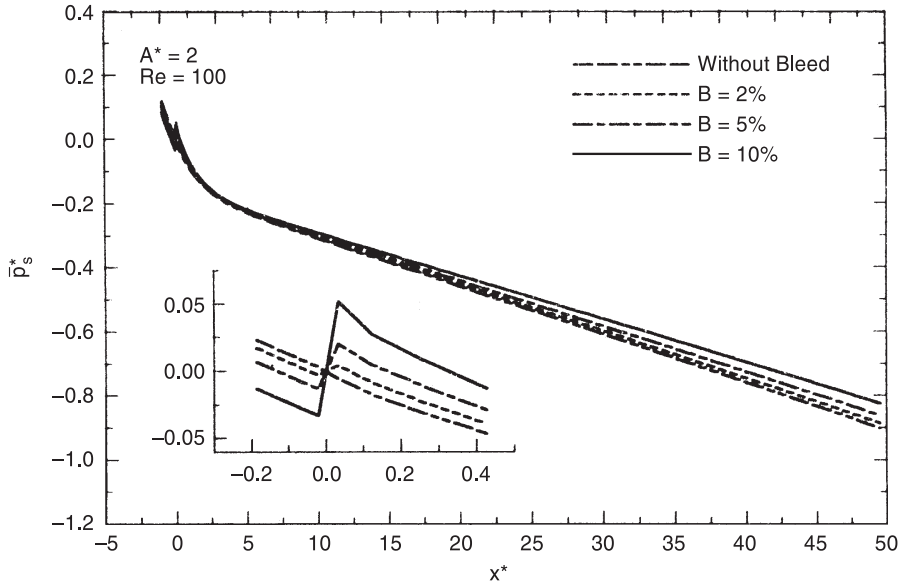

Figure 5.
Variation of average stagnation pressure with axial distance

average static pressure at any cross-section is determined by the following expression:

$$\bar{p} = \frac{\int p dA}{\int dA} \tag{5}$$

The variation of average static pressure along the diffuser length is described in Figure 6. In this figure, a fully developed inlet profile has been assumed while the area ratio and Reynolds number are held constant at 2 and 100 respectively. The amount of bleed represents the parameter. The most striking feature of this study is that it clearly delinates the advantages of VCD over the sudden expansion with no bleed as far as the peak of the static pressure rise curves are concerned. In fact, as the bleed is increased, a greater recovery of static pressure is achieved. This can be explained as follows: across the throat region, there is a sudden increase in area i.e. the denominator in the above expression increases sharply and presumably no amount of static pressure recovery across this region can compensate the steep fall of average static pressure at the throat. Then at the post-throat region, at a given section there are zones of positive pressure (due to fluid in the main stream that does not undergo recirculation) and negative pressure (due 10 recirculation). So the numerator is greatly affected by the presence of the negative pressure zone. Accordingly, the static pressure rise during this zone is small. As one moves

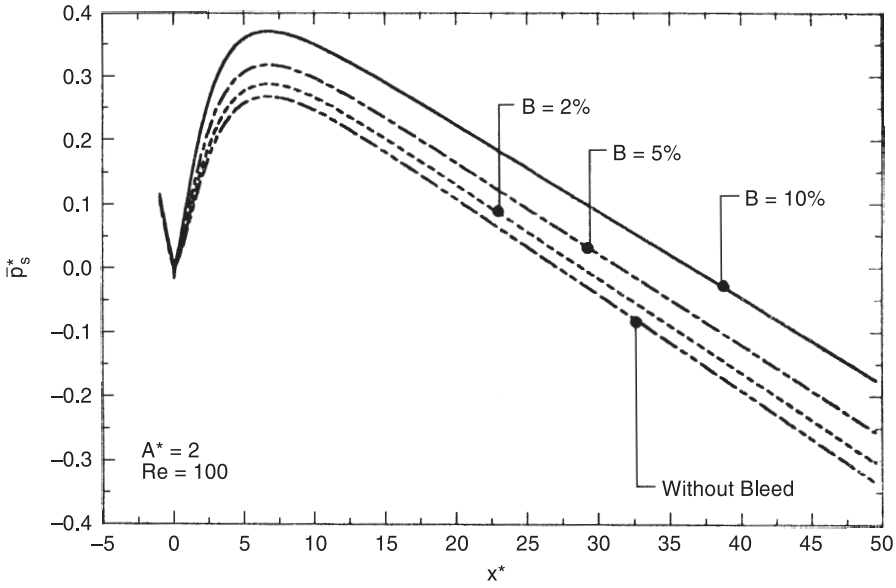

Figure 6.
Variation of average static pressure with axial distance

further downstream, the zone of positive pressure increases at the expense of the negative pressure zone; this in combination with the kinetic energy diffusion within the main stream, produces a significant pressure recovery. This same argument can be forwarded for all the three cases with the remarks that area of the negative pressure zone becomes smaller as the bleed is increased. Accordingly, a higher static pressure recovery is associated with a greater bleed.

Another important feature is that the location of the point of maximum pressure does not vary significantly during these test cases – an observation that deserves special introspection. Some typical flow patterns in the form of stream line maps are shown in Figures 7 and 8. It is evident from these figures that there exist three regimes of fluid flow – the first zone adheres to the vertical wall in the form of a closed loop, the second zone supplies the bleed fluid and the third zone containing the main fluid whose diffusion brings about the expected pressure rise. The second and third zones are separated by a divider stream line which stagnates on the outer wall of the VCD at a location which is dictated by Reynolds number. So, for the present case, in which bleed fraction is varied with constant Re, the said stream line manifests itself as the apparent boundary of a curved diffuser. Once the location of the stagnation point of the divider stream line is fixed by the value of Re, greater bleed results in smaller size of the closed loop region. However, this interaction between the first two zones seems to have little impact on the pressure recovery. Focussing the attention on the flow of main fluid, one notes from the stream line maps that

the stream lines are more packed along the centre line for 2 per cent bleed than for the 10 per cent bleed case i.e. a jet type flow occurs for lower bleed case. This does not result in a good static pressure recovery since majority of the stream lines because of the jet-like behaviour. does not conform to the diffuser shape. On the contrary, for a higher bleed case, the stream lines are loosely packed at the throat itself i.e. the flow velocity is decreased and the bulk of the fluid gets a chance to undergo the diffusion process.

3.5 Diffuser efficiency of VCD

Diffuser efficiency (η_{diffuser}) is a quantity of prime interest for the designer of diffusers. As the fluid undergoes the diffusion process in a VCD, the static pressure of the fluid increases. Hence, the diffuser efficiency represents a parameter which quantifies the increase of static pressure with respect to same ideal diffusion process. Identification of this ideal diffusion process seems to pose some problems as discussed below:

One way to define diffuser efficiency in non-dimensional form is:

$$\eta_{\text{diffuser}} = \frac{2\left(\bar{p}_2^* - \bar{p}_1^*\right)_{\text{measured}}}{\left(1 - \frac{1}{A^{*2}}\right)} \tag{6}$$

In this expression, $\bar{p}_2^*$ represents the maximum average static pressure achieved after the throat. The denominator represents the ideal static pressure rise in a sudden expansion, without any bleed, having an area ratio of A^*. The

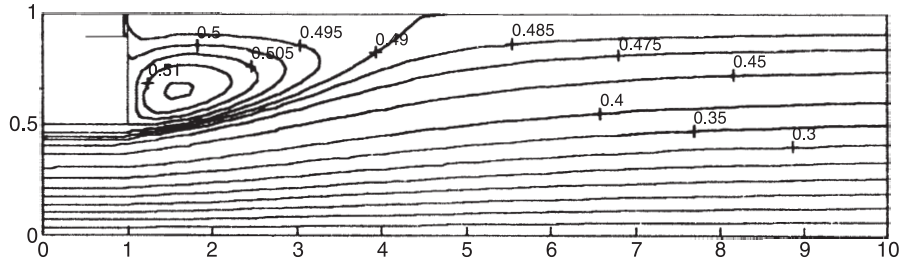

Figure 7.
Streamlines for $Re = 100$, $A^* = 2$, $B = 2$ per cent

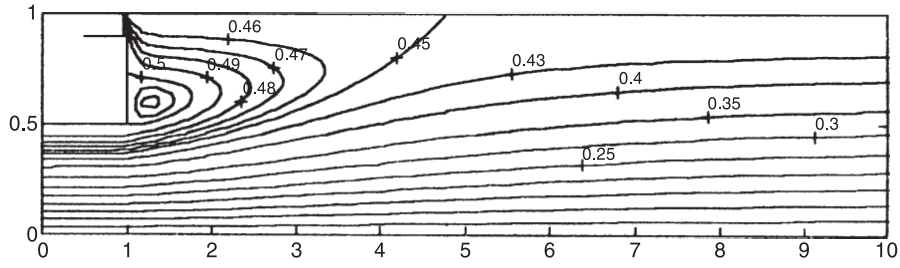

Figure 8.
Streamlines for $Re = 100$ $A^* = 2$, $B = 10$ per cent

significance of this expression for diffuser efficiency is that it quantifies the amount of static pressure rise with respect to the same for an ideal fluid passing through a sudden expansion. One of the serious shortcomings of this particular expression is that influence of such parameters as Re and bleed fraction does not exclusively appear in it.

Adkins, 1975, while carrying out an experimental work on VCD, proposed the following expression:

$$\eta_{\text{diffuser}} = \frac{2(\bar{p}_2^* - \bar{p}_1^*)_{\text{measured}}}{\left[1 - \frac{(1 - B^2)}{A^{*2}}\right]} \tag{7}$$

The striking feature of this expression is that it incorporates the bleed fraction (B) which is one of the most important parameter of a VCD. Moreover, when B is set equal to zero, it reduces to the earlier expression of diffuser efficiency. However, a careful look into the derivation of this expression reveals that while the bleed fraction was considered for satisfying continuity equation at two different planes within the diffuser, the same did not appear when the energy equation was considered. This then turns out to a source of a fatal error in its derivation and will not be considered any further in the present work. The earlier expression, in spite of its disadvantages cited above, is used in the present work because of its simplicity. This suggests that further discussion of diffuser efficiency should concentrate separately on its dependence on Reynolds number and bleed fraction.

The variation of η_{diffuser} on Re for different bleeds and aspect ratios is shown in Figure 9. In the preceeding section, we have established the reason behind the observation that with increase of bleed fraction, for a given Re and A^*, the maximum static pressure downstream of the throat increases. Now, for a given bleed fraction, it will be interesting to compare the performance of a VCD for different aspect ratios and Reynolds number. In general, it is observed that for lower values of A^*, for a given bleed fraction the VCD performs better as a diffuser with increase in Reynolds number. This is further reinforced by the observation that when there is no suction, the diffuser efficiency at a given Re decreases with increase in aspect ratio. Now, for sudden expansion without suction, as A^* increases, diffuser efficiency is expected to increase; however, at the same time the size of the recirculation eddy also increases implying an wasteful expenditure of fluid energy that could have otherwise been used up for static pressure gain. If this same reasoning is extended to the case of a VCD i.e. a sudden expansion with a given bleed fraction, it will be easy to see that the divider stream line leaves a greater zone of fluid on the other side of the main zone of diffusing fluid which ultimately puts an hold on the maximum value of $\bar{p}_2^*$. As a result, for the range of Reynolds number considered, one is set to conclude that if the performance of a VCD is based on diffuser efficiency, a VCD with smaller aspect ratio and increased bleed fraction would be a mare

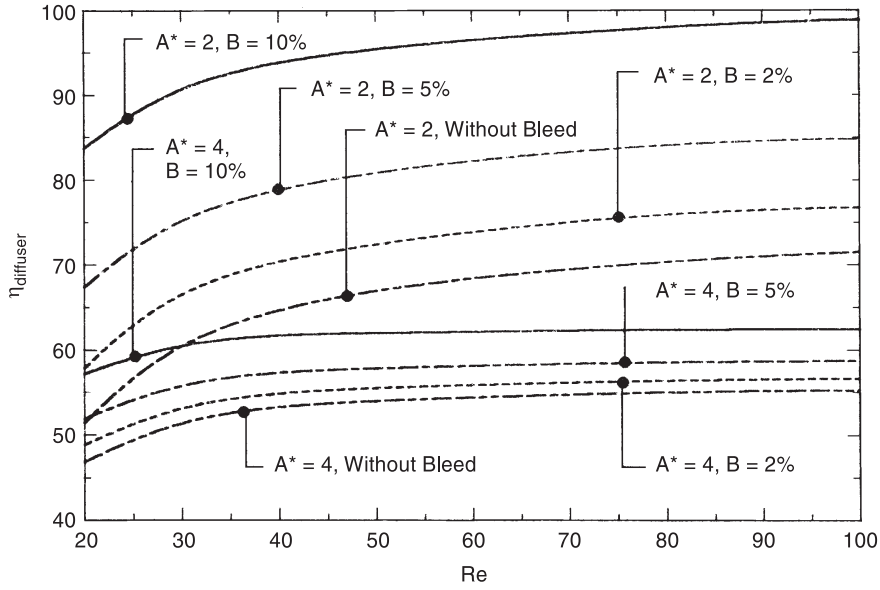

Figure 9.
Variation of diffuser efficiency with Reynolds number

preferred choice. Figure 10 shows the variation of η_{diffuser} with B for $A^* = 2$ and Re = 20 and 100. In each case a linear relationship exists for a given Re between η_{diffuser} and B. For steady sate operation of the VCD this is definitely a desirable feature.

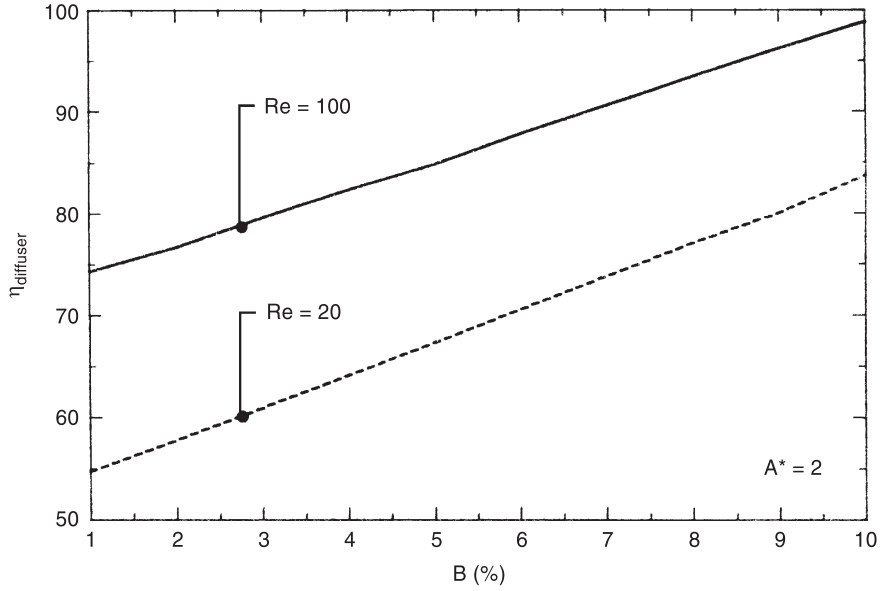

Figure 10.
Variation of diffuser efficiency with percentage of bleed

Effect of the variation of the position of the slot along the vertical side and the horizontal side, bleed fraction and the Reynolds number on the diffuser efficiency is quantitatively described in Table II. It is seen from the Table II, that as far as the position of suction slot along the vertical wall is concerned there is practically no effect on diffuser efficiency at lower bleed while at the higher bleed. best results are obtained by providing the slot at top of the vertical wall. Effect of the slot on the horizontal boundary on diffuser efficiency η_{diffuser} is also described in Table II. The figures in the bracket show the location of the stagnation point of the divider stream line. It is interesting to learn that the position of the slot almost dictates the position of the stagnation of the divider stream line; consequently, the apparent length and shape of the diffuser is greatly altered. For Re = 100, efficiency values increased as the distance of the slot from the upper corner is reduced from 10 to 5. Subsequent experiments on further reducing the distance from 5 to 2 resulted in only slight increase in the value of η_{diffuser} i.e., 74.26 per cent for 2 per cent bleed and 92.495 per cent for 10 per cent bleed. However, when the horizontal slot was located at the corner, the efficiency value was 77.83 per cent for 2 per cent bleed. For Re = 20 and for both the cases of 2 per cent and 10 per cent bleeds, the efficiency values have been noted to be less when the suction slot is placed on the horizontal wall, with respect to the corresponding efficiency values in case of suction slot located on the vertical wall. In general, then, a slot at the top corner is the most desirable location for the best performance of a VCD at least for the present Reynolds number regime.

4. Conclusion

In the resent study, a low Reynolds number performance simulation of a VCD has been carried out. The effects of important parameters like Area ratio, Re, Bleed fraction have been studied and the following features were revealed:

(1) In the presence of bleed, the VCD behaves in a completely different manner from that of a sudden expansion as far as the variation of total pressure along the diffuser is concerned.

		Position of suction slot on vertical wall			Position of suction slot on hoizontal wall		
Re	B (per cent)	Top	Middle	Bottom	$z^* = 2$	$z^* = 5$	$z^* = 10$
20	2	57.879	56.045	54.897	37.72	35.754	38.284
	10	83.724	74.76	69.858	47.766	35.738	38.391
100	2	76.75	76.552	75.994	74.26 (3.737)	73.11 (5.162)	69.513 (10.156)
	10	98.899	96.498	94.959	92.495 (4.127)	87.512 (5.43)	77.328 (10.23)

Table II. The efficiency of VCD for $A^* = 2$

(2) For a given aspect ratio and Reynolds number, the static pressure rise increases with increase in bleed.

(3) For the Reynolds number regime under consideration, it was observed that an area ratio of around two is most suitable. A similar observation was recorded earlier for the flow over a back step (Chakrabarti *et al.*).

(4) It has been established that the position of the bleed slot should be located preferably at the top corner of the VCD for the best performance. Location of the slot on the horizontal wall of the VCD is not recommended.

(5) For a given area ratio and Reynolds number, the diffuser efficiency increases linearly with increase in bleed fraction.

References

Adkins, R.C. (1975), "A short diffuser with low pressure loss", *ASME Jl. Fluids Engineering*, 93, pp. 297-302.

Beatty, C.G., "Diffuser control by trapped vortices", Thesis, Cranfield Institute of Technology, 1970.

Chakrabarti, S., Ray, S. and Sarkar, A., "Low Reynolds Number Flow through Sudden Expansion – From a Diffuser Viewpoint", To be communicated to elsewhere.

Heskestad, G. (1965), "An edge suction effect", *AIAA Journal*, 3, pp. 1958-61.

Heskestad, G. (1968), "A suction scheme applied to flow through sudden enlargement", *J. Basic Engineering, Trans. ASME, Series D*, 90, pp. 541-52.

Patankar, S.V. (1980), *Numerical Heat Transfer and Fluid Flow*, Hemisphere Publication.

Ringleb, F.O., "Flow control by generation of standing vortices and the cusp effect", AER No. 317, 1955, Princeton University.

Sullerey, R.K., Ashok, V. and Shantharam, K.V. (1992), "Effect of inlet flow distortion on performance of Vortex Controlled diffusers", *J. Fluids Engg., Trans. ASME*, 114, pp. 191-7.